Binary Image Registration Using Covariant Gaussian Densities

Csaba Domokos and Zoltan Kato

Department of Image Processing and Computer Graphics,
University of Szeged, P. O. Box 652., 6701 Szeged, Hungary
{dcs,kato}@inf.u-szeged.hu
http://www.inf.u-szeged.hu/~{dcs,kato}

Abstract. We consider the estimation of 2D affine transformations aligning a known binary shape and its distorted observation. The classical way to solve this registration problem is to find correspondences between the two images and then compute the transformation parameters from these landmarks. In this paper, we propose a novel approach where the exact transformation is obtained as a least-squares solution of a linear system. The basic idea is to fit a Gaussian density to the shapes which preserves the effect of the unknown transformation. It can also be regarded as a consistent coloring of the shapes yielding two rich functions defined over the two shapes to be matched. The advantage of the proposed solution is that it is fast, easy to implement, works without established correspondences and provides a unique and exact solution regardless of the magnitude of transformation.

1 Introduction

Image registration is an important step in almost all image processing tasks where images taken at different time, from different viewpoints, or under different modalities need to be compared or combined. Typical applications include image mosaicing, shape matching [1], super-resolution [2] or medical image analysis [3]. In a general setting, one is looking for a transformation which aligns two images such that one image (*template*) becomes similar to the second one (*observation*). There is a rich literature on registration methods, good surveys can be found in [4,5]. Most of these techniques contain the following four components: Easily detectable points of the *feature space* (*e.g.* line crossing, corners, etc.), called *landmarks*, used for establishing correspondences between the two images. For matching these points, a *similarity metric* is defined. The family of admissible transformations determines the *search space* and the goal is to find a transformation by minimizing the distance between the *template* and *observation*. Such methods are often called *feature-based*. Radiometric information usually plays a crucial role in establishing correspondences, while the aligning transformation is often found by the iterative closest point (ICP) algorithm [6]. However, since shapes are represented as binary images, radiometric information is not available in our case. As a result, the correspondence problem becomes

A. Campilho and M. Kamel (Eds.): ICIAR 2008, LNCS 5112, pp. 455–464, 2008.

quite challenging. One can only use geometric information but invariant geometric features (*e.g.* corners, junctions) might be difficult to extract (a circular shape, for instance). Another approach, called *area-based* registration, works without detecting landmarks. Instead, the problem is solved by computing global descriptors [7] or invariants of the objects [8,9]. Featureless methods [10,11] are able to compose, both geometrically and photometrically, a pair of uncalibrated images. A common problem with both approaches is that the solution requires an iterative optimization procedure. A novel segment-based shape matching algorithm is presented in [12] which avoids problems associated with purely global or local methods. This approach generalizes the idea of finding a point-to-point correspondence between two shapes to that of finding a segment-to-segment correspondence.

The parametric estimation of 2D affine transformations between *gray-level* images has been addressed in [13,14] where an accurate and computationally simple solution has been proposed avoiding both the correspondence problem as well as the need for optimization. The basic idea is to reformulate the original problem as an *equivalent linear parameter estimation* one which can be easily solved. This solution, however, makes use of the gray-level values which is not available in the binary case.

Herein, we will develop a novel method for registering *binary* images where the aligning transformation is restricted to the 2D *affine* group. We will show, that in spite of the missing radiometric information, we can still formulate the registration problem as the solution of a linear system of equations. The basic idea is to generate a pair of *covariant functions* that are related by the unknown transformation. The resulting algorithm is fast and provides a direct solution without making correspondences or optimization. The method has been tested on a large database of planar shapes. Experimental evidence suggests that our approach performs well both in terms of quality as well as in terms of computing time.

2 Problem Statement

Let us denote the coordinates of the *template* and *observation* points by $\mathbf{x} = [x_1, x_2]^T$, $\mathbf{y} = [y_1, y_2]^T \in \mathbb{R}^2$ respectively. The identity relation between the shapes is then as follows

$$\mathbf{y} = \mathbf{A}\mathbf{x} + \mathbf{t} \quad \Leftrightarrow \quad \mathbf{x} = \mathbf{A}^{-1}(\mathbf{y} - \mathbf{t}) = \mathbf{A}^{-1}\mathbf{y} - \mathbf{A}^{-1}\mathbf{t}, \tag{1}$$

where $(\mathbf{A}, \mathbf{t})$ is the unknown affine transformation that we want to recover. Classical landmark-based approaches would now identify at least 3 point pairs and solve the system of linear equations obtained from Eq. (1). However, we are interested in a direct solution without solving the correspondence problem. For that purpose, shapes will be represented by their characteristic function $\mathbb{1} : \mathbb{R}^2 \to \{0, 1\}$, where 0 and 1 correspond to the background and foreground

respectively. If we denote the *template* by $\mathbb{1}_t$ and the *observation* by $\mathbb{1}_o$, the following equality also holds

$$\mathbb{1}_t(\mathbf{x}) = \mathbb{1}_o(\mathbf{A}\mathbf{x}+\mathbf{t}) \quad \Leftrightarrow \quad \mathbb{1}_t(\mathbf{A}^{-1}(\mathbf{y}-\mathbf{t})) = \mathbb{1}_o(\mathbf{y}). \tag{2}$$

In addition, if we can observe some image features (*e.g.* gray-levels of the pixels [13,14]) that are invariant under the transformation $(\mathbf{A}, \mathbf{t})$, then we can define an additional relation

$$g(\mathbf{x}) = h(\mathbf{A}\mathbf{x}+\mathbf{t}) \quad \Leftrightarrow \quad g(\mathbf{A}^{-1}(\mathbf{y}-\mathbf{t})) = h(\mathbf{y}), \tag{3}$$

where $g, h : \mathbb{R}^2 \to \mathbb{R}$ are *covariant functions* under the transformation $(\mathbf{A}, \mathbf{t})$, defined on those observed features. Furthermore, the above relations are still valid when an *invariant function* $\omega : \mathbb{R} \to \mathbb{R}$ is acting on both sides of the equation [13,14]. Indeed, for a properly chosen ω

$$\omega(g(\mathbf{x})) = \omega(h(\mathbf{A}\mathbf{x}+\mathbf{t})) \quad \Leftrightarrow \quad \omega\big(g(\mathbf{A}^{-1}(\mathbf{y}-\mathbf{t}))\big) = \omega(h(\mathbf{y})).$$

The basic idea of [13,14] is to use nonlinear ω functions. This way, we can generate as many linearly independent equations as needed. Note that these equations doesn't contain new information, they simply impose new linearly independent constraints allowing for a unique solution.

3 Estimation of Distortion Parameters

The key idea of the proposed approach is to construct two *covariant functions* satisfying Eq. (3). Once this is achieved, we can adopt the direct method from [13,14] to solve for the unknown transformation $(\mathbf{A}, \mathbf{t})$. Since we do not have any radiometric information, this is a quite challenging task. We have to define these functions based on the only available geometric information.

3.1 Construction of Covariant Functions

We consider the points of the *template* as a sample from a bivariate normally distributed random variable $X \sim N(\mu, \Sigma)$. It is well known, that for any linear transformation, when $Y = \mathbf{A}X + \mathbf{t}$ then Y has also a bivariate normal distribution

$$X \mapsto Y \sim N(\mu', \Sigma') = N(\mathbf{A}\mu + \mathbf{t}, \mathbf{A}\Sigma\mathbf{A}^T).$$

Obviously, the above equation is only valid when $\mathbf{A}$ is non-singular and positive definite. In our case, $(\mathbf{A}, \mathbf{t})$ is an affine transformation thus $\mathbf{A}$ is clearly non-singular. On the other hand, a negative determinant would mean that the transformation is not orientation-preserving. In practice, however, such transformations are usually excluded by physical constraints. The parameters of the probability densities $N(\mu, \Sigma)$ and $N(\mu', \Sigma')$ can be easily estimated as the sample means and covariances (*i.e.* the mean and covariance of the point coordinates). From a geometric point of view, the mean values μ and μ' represent the

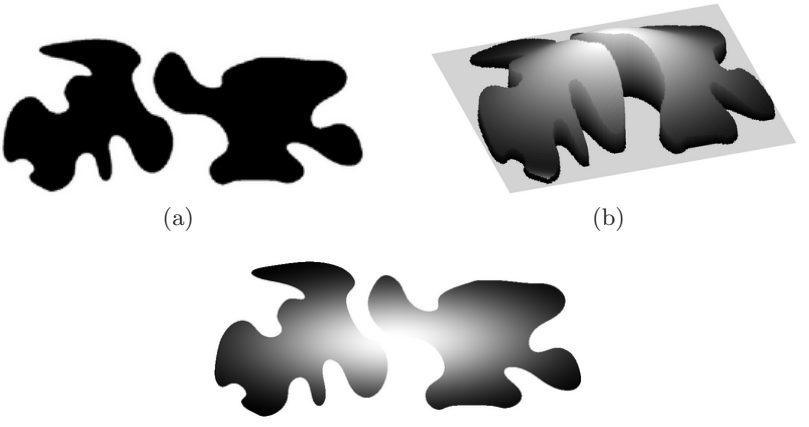

(a) (b)

(c)

Fig. 1. Gaussian density function fitted over the binary shape yields a consistent coloring. (a) Original binary image; (b) 3D plot of the Gaussian density function over the binary shape; (c) Gaussian density as a grayscale image.

center of mass of the *template* and *observation* respectively, while Σ and Σ' capture the orientation and eccentricity of the shapes. Fig. 1 shows a binary shape and the fitted Gaussian density.

Now let us examine the relationship between the bivariate Gaussian density functions p and p' computed from the *template* and *observation* respectively.

$$p'(\mathbf{y}) = \frac{1}{2\pi\sqrt{|\Sigma'|}} \exp\Big(-\frac{1}{2}(\mathbf{y}-\mu')^T \Sigma'^{-1}(\mathbf{y}-\mu')\Big).$$

Using $(\mathbf{y}-\mu') = (\mathbf{A}\mathbf{x}+\mathbf{t}-(\mathbf{A}\mu+\mathbf{t})) = (\mathbf{A}\mathbf{x}-\mathbf{A}\mu)$, we get

$$= \frac{1}{2\pi\sqrt{|\mathbf{A}\Sigma\mathbf{A}^T|}} \exp\Big(-\frac{1}{2}(\mathbf{A}\mathbf{x}-\mathbf{A}\mu)^T \mathbf{A}^{-T}\Sigma^{-1}\mathbf{A}^{-1}(\mathbf{A}\mathbf{x}-\mathbf{A}\mu)\Big)$$

$$= \frac{1}{2\pi|\mathbf{A}|\sqrt{|\Sigma|}} \exp\Big(-\frac{1}{2}(\mathbf{x}-\mu)^T \mathbf{A}^T\mathbf{A}^{-T}\Sigma^{-1}\mathbf{A}^{-1}\mathbf{A}(\mathbf{x}-\mu)\Big)$$

$$= |\mathbf{A}|^{-1}\frac{1}{2\pi\sqrt{|\Sigma|}} \exp\Big(-\frac{1}{2}(\mathbf{x}-\mu)^T \Sigma^{-1}(\mathbf{x}-\mu)\Big) = \frac{1}{|\mathbf{A}|}p(\mathbf{x}), \qquad (4)$$

where $|\mathbf{A}|$ can be easily expressed from $\mathbf{A}\Sigma\mathbf{A}^T = \Sigma'$ as

$$|\mathbf{A}||\Sigma||\mathbf{A}^T| = |\Sigma'|, \quad \text{hence} \quad |\mathbf{A}| = \sqrt{|\Sigma'|/|\Sigma|}. \qquad (5)$$

It is clear from Eq. (4) that p and p' are *covariant*. However, we can further simplify Eq. (4) by back substituting $|\mathbf{A}|$ into the equations and making necessary equivalent conversions, yielding

$$(\mathbf{x}-\mu)^T\Sigma^{-1}(\mathbf{x}-\mu) = (\mathbf{y}-\mu')^T\Sigma'^{-1}(\mathbf{y}-\mu'). \qquad (6)$$

In fact, we get the Mahalanobis-distance which defines a metric over the *template* and another transformed metric over the *observation*. We then define our *covariant functions* $P, S : \mathbb{R}^2 \to \mathbb{R}$ as

$$P(\mathbf{x}) = (\mathbf{x} - \mu)^T \Sigma^{-1} (\mathbf{x} - \mu) \quad \text{and} \quad S(\mathbf{y}) = (\mathbf{y} - \mu')^T \Sigma'^{-1} (\mathbf{y} - \mu'). \tag{7}$$

From Eq. (6)–(7), we get the desired relation of Eq. (3)

$$P(\mathbf{x}) = S(\mathbf{A}\mathbf{x} + \mathbf{t}) \quad \Leftrightarrow \quad P(\mathbf{A}^{-1}(\mathbf{y} - \mathbf{t})) = S(\mathbf{y}). \tag{8}$$

Note that both $P(\mathbf{x})$ and $S(\mathbf{y})$ can be computed directly from the input images. Fig. 2 shows an example of these functions fitted over a binary shape and its distorted observation.

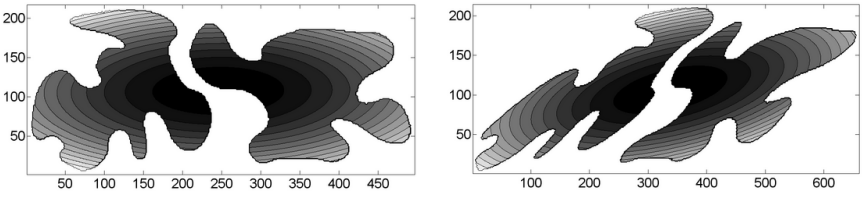

(a) (b)

Fig. 2. Mahalanobis-distance as *covariant function*. Level lines are overlayed on the original graylevel images for easier evaluation. (a) $P(\mathbf{x})\mathbb{1}_t(\mathbf{x})$: Mahalanobis-distance over the original image in Fig. 1. (b) $S(\mathbf{y})\mathbb{1}_o(\mathbf{y})$: Mahalanobis-distance over the transformed image. The transformation was a 1.5× shearing along the x-axis.

3.2 Linear Estimation of Affine Parameters

Since point correspondences are not available, we cannot construct a system directly from Eq. (8). However, multiplying Eq. (2) and Eq. (8), then integrating over $\mathbb{R}^2$ yields

$$\int_{\mathbb{R}^2} P(\mathbf{x})\mathbb{1}_t(\mathbf{x})d\mathbf{x} = \int_{\mathbb{R}^2} S(\mathbf{A}\mathbf{x} + \mathbf{t})\mathbb{1}_o(\mathbf{A}\mathbf{x} + \mathbf{t})d\mathbf{x} = |\mathbf{A}|^{-1} \int_{\mathbb{R}^2} S(\mathbf{y})\mathbb{1}_o(\mathbf{y})d\mathbf{y},$$

where we have used the integral transformation $\mathbf{x} = \mathbf{A}^{-1}(\mathbf{y} - \mathbf{t})$, $d\mathbf{x} = |\mathbf{A}|^{-1}d\mathbf{y}$. Since the characteristic functions take only values from $\{0, 1\}$, we can further simplify the above integrals by restricting them to the foreground regions $\mathcal{F}_t = \{\mathbf{x} \in \mathbb{R}^2 | \mathbb{1}_t(\mathbf{x}) = 1\}$ and $\mathcal{F}_o = \{\mathbf{y} \in \mathbb{R}^2 | \mathbb{1}_o(\mathbf{y}) = 1\}$

$$\int_{\mathcal{F}_t} P(\mathbf{x})d\mathbf{x} = \int_{\mathcal{F}_t} S(\mathbf{A}\mathbf{x} + \mathbf{t})d\mathbf{x} = \frac{1}{|\mathbf{A}|} \int_{\mathcal{F}_o} S(\mathbf{y})d\mathbf{y}.$$

This equation implies that the finite domains $\mathcal{F}_t$ and $\mathcal{F}_o$ are also related: $\mathbf{A}\mathcal{F}_t + \mathbf{t} = \mathcal{F}_o$, *i.e.* we match the shapes as a whole instead of point correspondences. It is clear that both sides of the equation as well as the Jacobian can be easily

computed from the input images. However, we need an equation which also contains the unknown elements of the affine transformation. This is easily achieved by multiplying both sides by $\mathbf{x}$. Furthermore, we need more than one linearly independent equation as we have 6 unknowns. For that purpose, we will adopt the idea from [13,14] and generate new equations by making use of appropriate *invariant functions* $\omega : \mathbb{R} \to \mathbb{R}$. Thus we get

$$\int_{\mathcal{F}_t} \mathbf{x}\omega(P(\mathbf{x}))d\mathbf{x} = \int_{\mathcal{F}_t} \mathbf{x}\omega(S(\mathbf{A}\mathbf{x}+\mathbf{t}))d\mathbf{x} = \frac{1}{|\mathbf{A}|}\int_{\mathcal{F}_o} \mathbf{A}^{-1}(\mathbf{y}-\mathbf{t})\omega(S(\mathbf{y}))d\mathbf{y}.$$

Note that in the last step, we have applied the integral transformation $\mathbf{x} = \mathbf{A}^{-1}(\mathbf{y}-\mathbf{t})$, $d\mathbf{x} = |\mathbf{A}|^{-1}d\mathbf{y}$. If q_{ki} denotes the elements of $\mathbf{A}^{-1}$ and $-\mathbf{A}^{-1}\mathbf{t}$, *i.e.*

$$\mathbf{A}^{-1} = \begin{pmatrix} q_{11} & q_{12} \\ q_{21} & q_{22} \end{pmatrix} \quad \text{and} \quad -\mathbf{A}^{-1}\mathbf{t} = \begin{pmatrix} q_{13} \\ q_{23} \end{pmatrix},$$

we can expand the integrals yielding the following linear system

$$|\mathbf{A}|\int_{\mathcal{F}_t} x_k\omega(P(\mathbf{x}))d\mathbf{x} = \sum_{i=1}^{2} q_{ki}\int_{\mathcal{F}_o} y_i\omega(S(\mathbf{y}))d\mathbf{y} \; + \; q_{k3}\int_{\mathcal{F}_o} \omega(S(\mathbf{y}))d\mathbf{y}, \; k = 1, 2.$$

Adopting a set of *invariant functions* $\{\omega_i\}_{i=1}^n$, we can write the linear system in matrix form

$$\begin{pmatrix} \int y_1\omega_1(S(\mathbf{y})) & \int y_2\omega_1(S(\mathbf{y})) & \int \omega_1(S(\mathbf{y})) \\ \vdots & \vdots & \vdots \\ \int y_1\omega_n(S(\mathbf{y})) & \int y_2\omega_n(S(\mathbf{y})) & \int \omega_n(S(\mathbf{y})) \end{pmatrix} \begin{pmatrix} q_{k1} \\ q_{k2} \\ q_{k3} \end{pmatrix} = |\mathbf{A}| \begin{pmatrix} \int x_k\omega_1(P(\mathbf{x})) \\ \vdots \\ \int x_k\omega_n(P(\mathbf{x})) \end{pmatrix}, \tag{9}$$

where $k = 1, 2$ and $\int f(x)$ denotes the integral computed over the corresponding finite domain $\mathcal{F}_t$ or $\mathcal{F}_o$. The solution of this linear system provides the parameters of the registration. If $n > 3$ then the system is over-determined and the solution is obtained as a least squares solution. As shown by Hagege and Francos [13,14], when the object is not affine symmetric, then this solution is unique. Note that independently of the number of systems, the coefficient matrix need to be computed only once. Hence the complexity of the algorithm depends linearly on the size of the objects.

4 Experimental Results

We have constructed our equations in the continuum but in practice we only have a limited precision digital image. Hence the integral over the domains $\mathcal{F}_t$ and $\mathcal{F}_o$ can only be *approximated* by a discrete sum over the foreground pixels. Clearly, the resolution of the images affects the precision of this approximation. As the mesh size tends to zero, the finite sums approximate better the integral. Therefore our method performs better on higher resolution images. However, due to its linear time complexity, the proposed algorithm runs quite fast on

large images thus we do not have to compromise quality when CPU time is critical.

Theoretically any *invariant function* could be applied for constructing the system in Eq. (9). In practice, however the registration result depends on the set of ω because of the inherent errors due to discretization. In our experiments, we found that the following set of functions gives good results (see Fig. 3): x, $\cos(x)$, $\cos(2x)$, $\sin(x)$ and $\sin(2x)$.

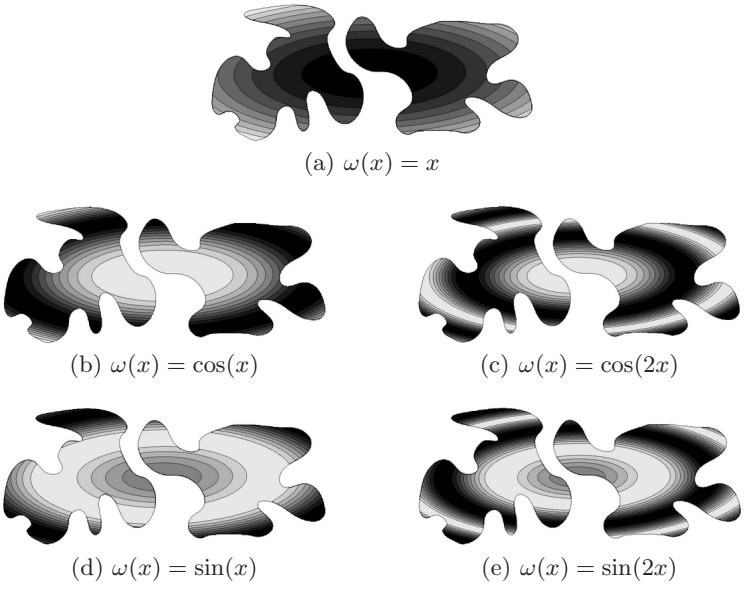

(a) $\omega(x) = x$

(b) $\omega(x) = \cos(x)$ (c) $\omega(x) = \cos(2x)$

(d) $\omega(x) = \sin(x)$ (e) $\omega(x) = \sin(2x)$

Fig. 3. The effect of the applied ωs on the image in Fig. 1. Level lines are overlayed on the original graylevel images for easier evaluation.

In order to analyze the performance of our algorithm, we have created an image dataset containing 1000 synthetically generated observations for 37 different binary shapes. The applied transformations were randomly composed of $0°, 60°, \ldots, 240°$ rotations; $0, 0.5, 1$ shearings; $0, 0.5, \ldots, 2$ scalings, and $0, 20$ translations along both axes. The algorithm has been implemented in Matlab 7.2 and ran on a SunFire V490 with 8192MB memory under Solaris 10. The average runtime was around 1.5 seconds per image of size 1000×1000. It is clear from the formulation of Algorithm 1 that its time complexity is $\mathcal{O}(N)$, where N is the number of foreground pixels.

In order to compare registration results, we evaluated two kind of error measures for each estimated transformation $(\widehat{\mathbf{A}}, \widehat{\mathbf{t}})$. Since we know the applied transformation for each synthetic example, we can evaluate the distance (denoted by ϵ) between the transformed version of the template by $(\mathbf{A}, \mathbf{t})$ (*observation*) and by $(\widehat{\mathbf{A}}, \widehat{\mathbf{t}})$ (*registered*) based on all template points $\mathbf{x}$. Another measure is the

Algorithm 1. Pseudo-code of the proposed algorithm. Note that there is no iterative step, it provides the solution in a single pass.

input : The *template* ($\mathbb{1}_t$) and *observation* ($\mathbb{1}_o$)
output: Estimated affine transformation $(\widehat{\mathbf{A}}, \widehat{\mathbf{t}})$

1 Computing the sample means μ, μ' and covariances Σ, Σ' from the points of the foreground objects
2 Constructing the *covariant function*s using Eq. (7):
$P, S : \mathbb{R}^2 \to \mathbb{R},\ \mathbf{x} \mapsto (\mathbf{x}-\mu)^T \Sigma^{-1}(\mathbf{x}-\mu)$
3 Choosing a set of *invariant function*s $\{\omega_i\}_{i=1}^n$, $n \geq 3$
4 Estimating the Jacobian $|\mathbf{A}|$ using Eq. (5)
5 Constructing the system of linear equations Eq. (9)
6 Solving the system (with least squares when $n > 3$) gives $(\widehat{\mathbf{A}}^{-1}, -\widehat{\mathbf{A}}^{-1}\widehat{\mathbf{t}}\ )$

absolute difference (denoted by δ) between the *observation* and the *registered* image.

$$\epsilon = \frac{1}{m} \sum_{\mathbf{x}} \frac{\|(\mathbf{A}-\widehat{\mathbf{A}})\mathbf{x} + \mathbf{t} - \widehat{\mathbf{t}}\|}{\|\mathbf{A}\mathbf{x}+\mathbf{t}\|}, \quad \text{and} \quad \delta = \frac{|R \triangle O|}{|R| + |O|} \times 100\%,$$

where m is the number of *template* pixels, $\triangle$ denotes the symmetric difference, while R and O denote the set of pixels of the *registered* image and *observation* respectively. The smaller these numbers are, the better is the matching. In summary, these measures give a quantitative characterization of the difference between the true transformation $(\mathbf{A}, \mathbf{t})$ and the estimated $(\widehat{\mathbf{A}}, \widehat{\mathbf{t}})$. Fig. 4 shows a registration result , where the true $(\mathbf{A})$ and estimated $(\widehat{\mathbf{A}})$ transformations were

$$\mathbf{A} = \begin{pmatrix} \cos(\frac{\pi}{9}) & \sin(\frac{\pi}{9}) \\ -\sin(\frac{\pi}{9}) & \cos(\frac{\pi}{9}) \end{pmatrix} \begin{pmatrix} 1.2 & 0.3 \\ 1.2 & 0.8 \end{pmatrix} = \begin{pmatrix} 1.538 & 0.5555 \\ 0.7172 & 0.6491 \end{pmatrix},$$

$$\widehat{\mathbf{A}} = \begin{pmatrix} 1.5266 & 0.5374 \\ 0.7116 & 0.6389 \end{pmatrix}.$$

4.1 Comparison to Previous Approaches

A recent approach for binary registration of images has been presented in [15]. In fact, the method addresses the registration of images taken under very different lighting conditions or in different seasons. Hence it is not possible to directly measure an invariant image feature as shown in Eq. (3). To overcome this difficulty, the authors extract edges from the images and compute some statistics of the edges which is used as a similarity metric for matching features. Although we address a different problem, this approach demonstrates the importance of the registration of *binary* images. In many cases, the variability of the object signatures is so complex that the only feasible way to register such images is to reduce them to a binary representation and solve the registration problem in that context.

(a) (b)

Fig. 4. Registration result. (a) Distorted *observation* of the sample image in Fig. 1 (rotated, scaled and sheared). (b) Registration result of the proposed method. The image is obtained by applying the recovered inverse transformation to the *observation*. The registration error was $\delta = 0.95\%$ and $\epsilon = 1.59$ pixel.

Probably the most closely related approach is the binary registration algorithm proposed by Kannala *et al.* [8]. The fundamental difference is that [8] constructs a system of equations by looking at the images at 3 different scales. Although the resulting system is also linear, the solution is inherently less precise as in each equation they can only use part of the available information. On the other hand, our approach constructs the equations by making use of the *invariant functions* ω hence we always use all the information available in the images. We have obtained the Matlab implementation from the authors and conducted a comparative test on our dataset. The results presented in Table 1 show that our method outperforms [8] in both quality and computing time.

Table 1. Registration results on 1000 images. We show the median of the error measures and the runtimes for each method.

Method	ϵ (pixels)	δ (%)	CPU time (sec.)
Proposed method	5.42	2.6	1.5
Kannala *et al.* [8]	50.92	21.46	107.19

5 Conclusion

In this paper, we have presented a novel approach for binary image registration. The fundamental difference compared to classical image registration algorithms is that our method works without any landmark extraction, correspondence, or iterative optimization. It makes use of all the information available in the input images and constructs a linear system of equations which can be solved easily. Although we only considered affine transformations, other commonly used linear transformations, like rigid-body or Euclidean, are special cases of the affine family. The complexity of the algorithm is linear hence it is potentially capable of registering images at near real-time speed.

References

1. Belongie, S., Malik, J., Puzicha, J.: Shape matching and object recognition using shape context. IEEE Transactions on Pattern Analysis and Machine Intelligence 24(4), 509–522 (2002)
2. Vandewalle, P., Sbaiz, L., Süsstrunka, S., Vetterli, M.: Registration of aliased images for super-resolution imaging. In: Visual Communications and Image Processing Conference. SPIE Proceedings, San Jose, CA, USA, vol. 6077, pp. 13–23 (2006)
3. Maintz, J.B.A., Viergever, M.A.: A survey of medical image registration. Medical Image Analysis 2(1), 1–36 (1998)
4. Brown, L.G.: A survey of image registration techniques. ACM Computing Surveys 24(4), 325–376 (1992)
5. Zitová, B., Flusser, J.: Image registration methods: A survey. Image and Vision Computing 21(11), 977–1000 (2003)
6. Besl, P.J., McKay, N.D.: A method for registration of 3-D shapes. IEEE Transactions on Pattern Analysis and Machine Intelligence 14(2), 239–256 (1992)
7. Flusser, J., Suk, T.: A moment-based approach to registration of images with affine geometric distortion. IEEE Transactions on Geoscience and Remote Sensing 32(2), 382–387 (1994)
8. Kannala, J., Rahtu, E., Heikkilä, J., Salo, M.: A new method for affine registration of images and point sets. In: Kalviainen, H., Parkkinen, J., Kaarna, A. (eds.) SCIA 2005. LNCS, vol. 3540, pp. 224–234. Springer, Heidelberg (2005)
9. Heikkilä, J.: Pattern matching with affine moment descriptors. Pattern Recognition 37(9), 1825–1834 (2004)
10. Mann, S., Picard, R.W.: Video orbits of the projective group a simple approach to featureless estimation of parameters. IEEE Transactions on Image Processing 6(9), 1281–1295 (1997)
11. Aguiar, P.M.Q.: Unsupervised simultaneous registration and exposure correction. In: Proceedings of International Conference on Image Processing, Atlanta, GA, USA, pp. 361–364. IEEE, Los Alamitos (2006)
12. McNeill, G., Vijayakumar, S.: Hierarchical procrustes matching for shape retrieval. In: Werner, B. (ed.) Proceedings of Computer Vision and Pattern Recognition, New York, vol. 1, pp. 885–894. IEEE, Los Alamitos (2006)
13. Hagege, R., Francos, J.M.: Parametric estimation of multi-dimensional affine transformations: An exact linear solution. In: Proceedings of International Conference on Acoustics, Speech, and Signal Processing, Philadelphia, USA, vol. 2, pp. 861–864. IEEE, Los Alamitos (2005)
14. Hagege, R., Francos, J.M.: Linear estimation of sequences of multi-dimensional affine transformations. In: Proceedings of International Conference on Acoustics, Speech and Signal Processing, Toulouse, France, vol. 2, pp. 785–788. IEEE, Los Alamitos (2006)
15. Simonson, K.M., Drescher, S.M., Tanner, F.R.: A statistics-based approach to binary image registration with uncertainty analysis. IEEE Transactions on Pattern Analysis and Machine Intelligence 29, 112–125 (2007)